

Flexoelectricity-Driven Mechanical Switching of Polarization in Metastable Ferroelectrics


Ji Hye Lee^{1,2,*}, Hong Joon Kim,^{1,2} Jiyong Yoon,³ Sanghyeon Kim,³ Jeong Rae Kim,^{1,2} Wei Peng,^{1,2}
Se Young Park,^{4,†} Tae Won Noh,^{1,2} and Daesu Lee^{3,‡}

¹*Center for Correlated Electron Systems, Institute of Basic Science, Seoul 08826, Korea*

²*Department of Physics and Astronomy, Seoul National University, Seoul 08826, Korea*

³*Department of Physics, Pohang University of Science and Technology, Pohang 37673, Korea*

⁴*Department of Physics and Origin of Matter and Evolution of Galaxies (OMEG) Institute, Soongsil University, Seoul 06978, Korea*

 (Received 25 October 2021; revised 29 April 2022; accepted 26 July 2022; published 8 September 2022)

Flexoelectricity-based mechanical switching of ferroelectric polarization has recently emerged as a fascinating alternative to conventional polarization switching using electric fields. Here, we demonstrate hyperefficient mechanical switching of polarization exploiting metastable ferroelectricity that inherently holds a unique mechanical response. We theoretically predict that mechanical forces markedly reduce the coercivity of metastable ferroelectricity, thus greatly bolstering flexoelectricity-driven mechanical polarization switching. As predicted, we experimentally confirm the mechanical polarization switching via an unusually low mechanical force (100 nN) in metastable ferroelectric CaTiO₃. Furthermore, the use of low mechanical forces narrows the width of mechanically writable nanodomains to sub-10 nm, suggesting an ultrahigh data storage density of ≥ 1 Tbit cm⁻². This Letter sheds light on the mechanical switching of ferroelectric polarization as a viable key element for next-generation efficient nanoelectronics and nanoelectromechanics.

DOI: [10.1103/PhysRevLett.129.117601](https://doi.org/10.1103/PhysRevLett.129.117601)

Ferroelectrics comprise a class of materials with spontaneous polarization that is switchable by external excitations, including electrical bias [1] and the chemical environment [2]. Polarization switching has been the basis for various device applications (e.g., nonvolatile memories and field-effect transistors [3]), but may have greater potential in complex ferroelectrics. Notably, complex ferroelectrics characteristically exhibit rich coupling between polarization and other degrees of freedom, allowing magnetoelectric switching [4] or scale-free ferroelectricity [5]. This coupling could also result in multiple competing states, thus lowering the effective energy barrier for polarization switching [6,7]. Therefore, proper control of polarization switching in complex ferroelectrics would maximize its application potential (e.g., by enabling energy-efficient device operation).

Recently, an exciting new concept based on flexoelectricity [8–11] has emerged, which uses mechanical forces to switch ferroelectric polarization [12]. This so-called mechanical polarization switching usually adopts an atomic force microscope (AFM) geometry [inset of Fig. 1(a)]. The mechanical loading force (F_L) by the AFM tip can generate strain gradients $\partial\epsilon/\partial x$ as large as $10^6 - 10^7$ m⁻¹ near the tip-sample contact region. Then, an effective flexoelectric field (i.e., $E_{\text{eff}}^{\text{flexo}} = f\partial\epsilon/\partial x$, where f is the flexocoupling coefficient) arises and could switch the polarization in ultrathin ferroelectrics. While this AFM tip-driven flexoelectricity has attracted a wide range of scientific interest [12–18], the associated mechanical polarization switching

could also be technologically advantageous. In particular, it can minimize electrical bias-induced side effects, such as charge injection, Joule heating, and dielectric breakdown. In addition, mechanically written nanodomains may be spatially denser than their electrically induced counterparts [12,19], while exhibiting comparable response time and retention properties [20,21].

However, wide and practical application of mechanical polarization switching requires considerable effort to lower the required F_L and enable higher-density nanodomain writing. There have been a few previous attempts to reduce the threshold F_L for mechanical polarization switching [19,34–36]. A simple method involves the use of a material that has low ferroelectric coercivity [34,35]. However, this inevitably increases the critical size of stable nanodomains [37] and could limit the ultimate data storage density. Another approach is to explore soft materials, such as ferroelectric polymers [19,36], which have a low elastic modulus and can therefore hold large strain gradients despite low F_L . According to contact mechanics theory [33], however, the low elastic modulus concurrently increases the tip-sample contact area, thereby limiting the achievable density of mechanically written domains. Thus, previous attempts to lower the threshold F_L have seemed innately incompatible with higher-density nanodomain writing, posing a difficult dilemma. In this Letter, we overcome this dilemma by utilizing a unique mechanical response of metastable ferroelectricity in a complex material.

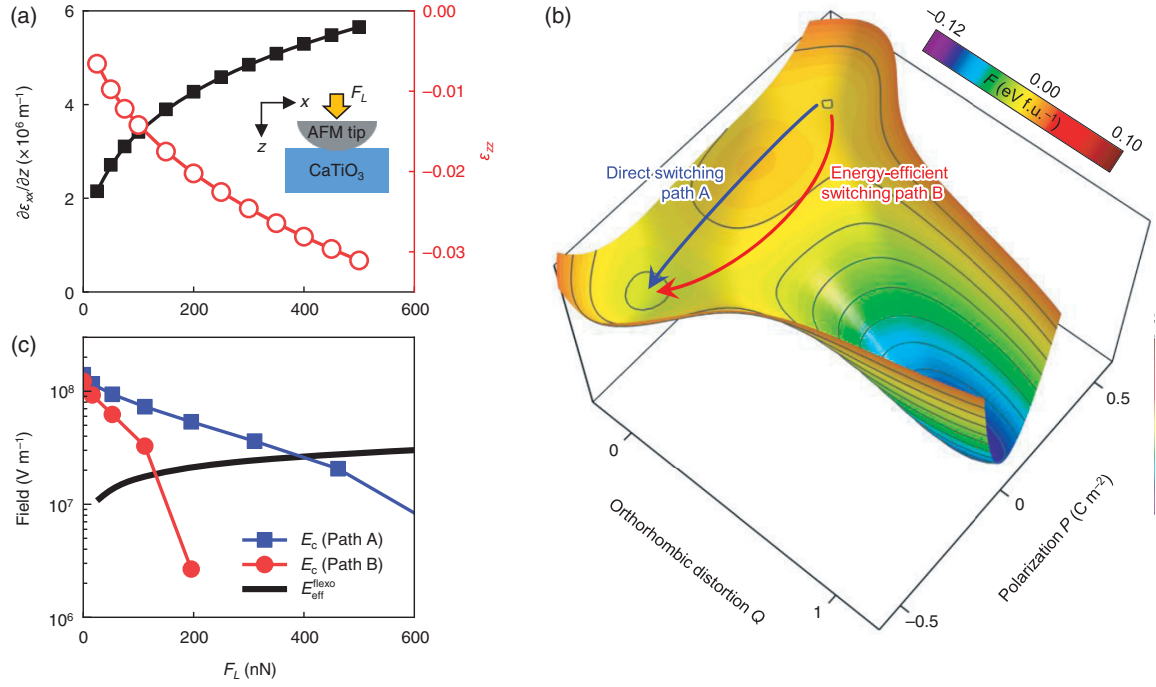


FIG. 1. Mechanical response of metastable ferroelectricity. (a) Transverse strain gradient $\partial \epsilon_{xx} / \partial z$ (black closed squares) and longitudinal strain ϵ_{zz} (red open circles) as a function of the applied AFM tip loading forces (F_L). The spatial distribution of strains induced by AFM tip loading is analytically calculated with the Hertzian contact model and Boussinesq's equation (Supplemental Material Note A [22]) [15,33]. (b) Free energy landscape of CaTiO_3 under a certain E_{eff} . There exists an energy-efficient switching path with a smaller energy barrier (red line), compared with the direct switching path (blue line). (c) Coercive field (E_c) as a function of the applied F_L , estimated for the direct switching path (blue closed squares) and energy-efficient switching path (red closed circles). We assume a thermal fluctuation of 0.7 meV (Supplemental Material Note C [22]). In estimating E_c , we only consider the effect of the strain ϵ_{zz} by F_L ; that is, the explicit contribution from the strain gradient (by F_L) in Eq. (1) is omitted, and we assume a general field for E_{eff} (Supplemental Material, Note C [22]). The effect of the strain gradient by F_L is separately treated for the flexoelectric field. The black line denotes the effective flexoelectric field [i.e., $E_{\text{eff}}^{\text{flexo}} = f(\partial \epsilon_{xx} / \partial z + \partial \epsilon_{yy} / \partial z)$, where f is the flexocoupling coefficient] as a function of the applied loading forces; f is typically in the range of 1–10 V [8,11], and we assume $f = 2.5$ V for CaTiO_3 , comparable to the value observed for SrTiO_3 (i.e., 2.6 V) [9].

We note that under the AFM tip-induced F_L , the sample experiences considerable longitudinal compressive strain, as well as a strain gradient [Fig. 1(a) and Supplemental Material Fig. S1]. Therefore, although ferroelectric coercivity is initially large, it could be reduced by the AFM tip-induced longitudinal compressive strain [Figs. 1(b) and 1(c)] [20]. Such a decrease in ferroelectric coercivity is key to efficient mechanical polarization switching using AFM geometry. We propose that exploiting metastable ferroelectricity would maximize this benefit: when a ferroelectric state is metastable, the AFM tip-induced strain could more substantially reduce the ferroelectric coercivity. Therefore, in metastable ferroelectrics, we envisage hyperefficient mechanical polarization switching operable with low F_L , without compromising the density of written nanodomains.

As a relevant metastable ferroelectric system, we adopt CaTiO_3 thin films. Recently, we theoretically and experimentally demonstrated metastable ferroelectricity at room temperature in (111)-oriented CaTiO_3 thin films [38]. While CaTiO_3 bulk is nonpolar with an orthorhombic

($Pnma$) structure, the (111)-oriented heterostructure leads to artificial metastable ferroelectricity with rhombohedral ($R3c$) structure in CaTiO_3 . The metastable state is defined as the one located at a local energy minimum (not a global minimum), but the metastable ferroelectricity itself does not mean that it has a poor polarization strength or stability; in fact, our previous work evidenced a strong ferroelectricity of $R3c$ CaTiO_3 [38]. We can phenomenologically describe CaTiO_3 with two order parameters, P and Q , which correspond to polarization (from $R3c$) and orthorhombic distortion (from $Pnma$) (Supplemental Material, Fig. S2 [22]), respectively, and usually compete with each other [38]. Further considering the AFM tip-induced longitudinal compressive strain ϵ_{zz} (i.e., $\epsilon_{zz} < 0$), we construct the free energy as follows:

$$F = -\frac{\alpha_2}{2} P^2 + \frac{\alpha_4}{4} P^4 - \frac{\beta_2}{2} Q^2 + \frac{\beta_4}{4} Q^4 + \frac{\gamma}{2} P^2 Q^2 - \frac{\eta}{2} \epsilon_{zz} P^2 + \frac{\zeta}{2} \epsilon_{zz} Q^2 - P E_{\text{eff}}, \quad (1)$$

where we determine the coefficients based on first-principles density functional theory (DFT) calculations for bulk CaTiO_3 (see Supplemental Material, Note B [22]) and E_{eff} indicates an external effective electric field, originating from electric bias or strain gradient. The two terms $(-\eta/2)\epsilon_{zz}P^2$ and $(+\zeta/2)\epsilon_{zz}Q^2$ in Eq. (1) describe the responses of P and Q , respectively, to the applied ϵ_{zz} . The other possible nonpolar states are located energetically higher than $R3c$ and also would have little energetic interaction with E_{eff} . Thus, to the first-order approximation, we can consider only the two states, i.e., $Pnma$ and $R3c$, for addressing the polarization switching process under E_{eff} .

Figure 1(b) depicts the free energy landscape of CaTiO_3 under a certain E_{eff} , presenting the metastable ferroelectric (i.e., $P \neq 0$ and $Q = 0$) and $Pnma$ (i.e., $P = 0$ and $Q = 1$) states. Applying a sufficient E_{eff} into metastable ferroelectric CaTiO_3 would lead to a transition from one polarization state to another, rather than the most stable $Pnma$ state. This is based on Ostwald's step rule [39,40], which explains that a phase transition may end with a metastable phase with free energy close to that of the parent phase, rather than the most stable phase. Also, it should be noted that our DFT calculations were performed in bulk CaTiO_3 , so there should be an additional influence from the underlying substrate, which favors the $R3c$ ferroelectric phase but is not included in Eq. (1). This additional influence, along with the Ostwald's step rule, will help prevent CaTiO_3 from falling into the $Pnma$ state during ferroelectric polarization switching. Then, polarization switching could occur through a detour path with a much lower energy barrier [red line in Fig. 1(b)], compared with the direct switching path [blue line in Fig. 1(b)]. Such an energy-efficient switching path stems from "metastable" ferroelectricity and could vastly facilitate mechanical polarization switching, as discussed below.

Using the phenomenological model based on DFT calculations, we estimate the threshold F_L for polarization switching in metastable ferroelectric CaTiO_3 . Considering thermally assisted polarization switching at finite temperatures [41], we find that F_L -induced compressive ϵ_{zz} could markedly reduce ferroelectric coercivity [Fig. 1(c) and Supplemental Material, Note C [22]]. In contrast, $E_{\text{eff}}^{\text{flexo}}$ tends to grow with F_L , eventually exceeding ferroelectric coercivity at a specific F_L ; polarization switching occurs at this threshold F_L . The estimated threshold F_L is around 130 nN, which is much smaller than in the case of the direct switching path (around 400 nN) or other conventional ferroelectrics (around 500 nN) [12,34,35]. Furthermore, the low threshold F_L could guarantee mechanical writing of ultrahigh-density ferroelectric nanodomains due to the decreased tip-sample contact area [33]. Notably, even if ferroelectric coercivity decreases significantly with the applied F_L , it is initially $>10^8 \text{ V m}^{-1}$, large enough to ensure the stability of mechanically written nanodomains. Therefore, metastable ferroelectric CaTiO_3 could exhibit

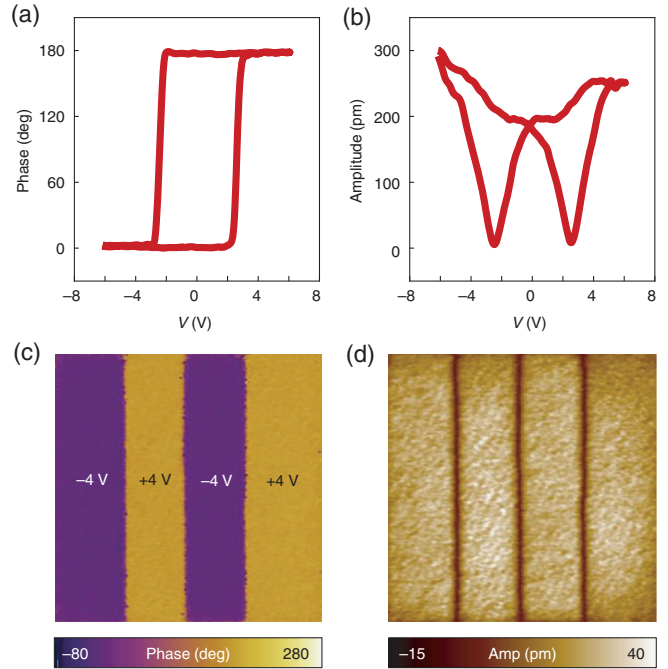


FIG. 2. Local ferroelectric characterization of CaTiO_3 (111) films by PFM. (a) and (b) Local hysteresis curves of phase vs voltage (a) and amplitude vs voltage (b). (c) and (d) PFM phase (c) and amplitude (d) images of bipolar polarization states. Image scan size: $2 \times 2 \mu\text{m}^2$.

enhanced mechanical polarization switching that satisfies both low threshold F_L and high-density nanodomain writing.

To examine this intriguing possibility, we fabricated epitaxial CaTiO_3 thin films on LaAlO_3 (111) single crystal substrate with a buffer layer LaNiO_3 as a bottom electrode by pulsed laser deposition. First, we conduct electrical and mechanical switching of ferroelectric polarization in CaTiO_3 using a piezoresponse force microscope (PFM). All the experimental details and methods are in the methods section of Supplemental Material [22]. We first examine the typical electrical switching behaviors of ferroelectric polarization in 5 nm-thick CaTiO_3 (111) films (Fig. 2). To minimize any mechanical force effect during electrical switching, we carry out the experiments in Fig. 2 with a low F_L (i.e., 30 nN). We then investigate mechanical polarization switching by scanning the sample with a tip under a higher F_L while turning off the external electric field. Importantly, although the coercive voltage of CaTiO_3 is initially high [i.e., 2.5 V; Fig. 2(a)], applying a slightly increased F_L reverses the upward polarization downward (Fig. 3). Based on PFM phase and amplitude line profiles, we estimate the threshold F_L for polarization switching to be as small as 100 nN [Figs. 3(c) and 3(d)]. By exploring the polarization switching hysteresis as a function of F_L , we also confirm the low threshold F_L of around 100 nN (Supplemental Material, Fig. S8 [22]). The measured low threshold F_L quantitatively agrees with our predictions

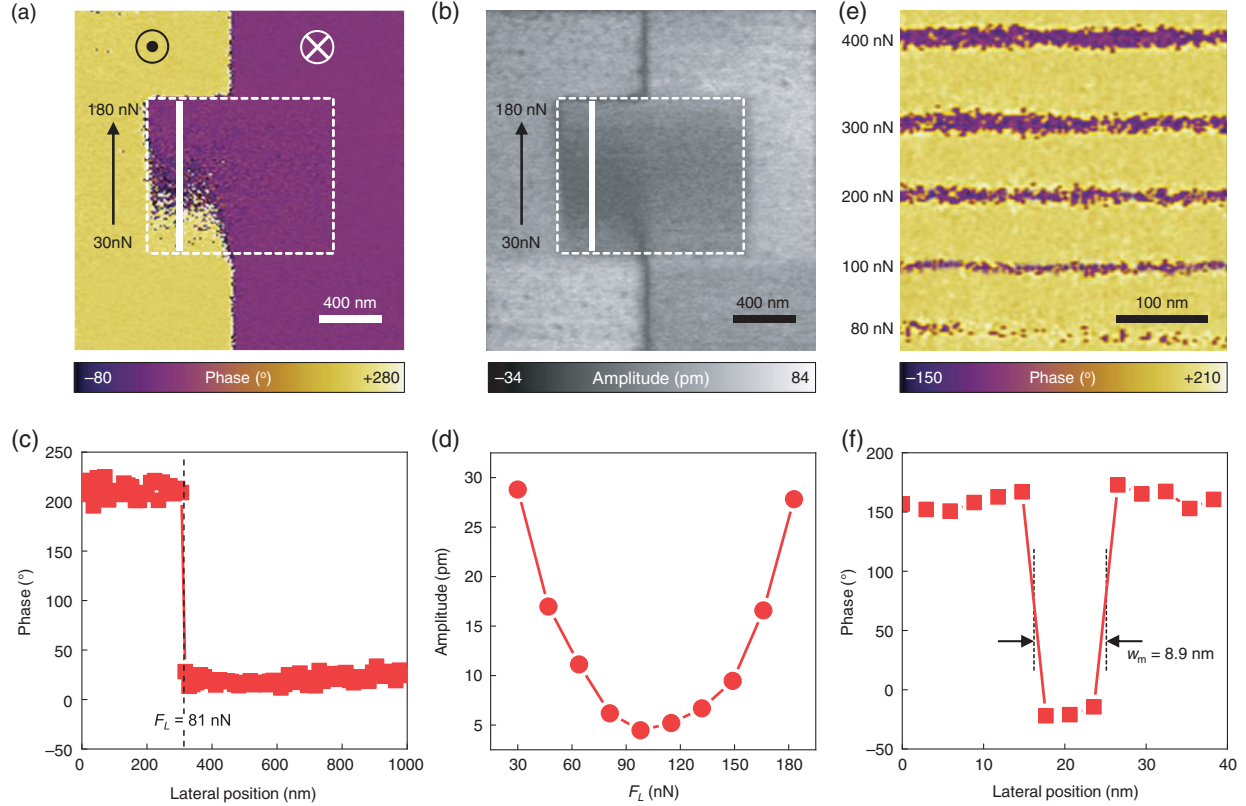


FIG. 3. Mechanical switching in CaTiO_3 (111) films. (a) and (b) PFM phase (a) and amplitude (b) images after mechanical writing of polarization. After bistable polarization domains are electrically written, a $1.2 \times 1.0\text{-}\mu\text{m}^2$ area (represented by the white dashed box) is scanned with the tip under incrementally increased force. F_L increases from bottom to top, as denoted by the black vertical arrow in (a) and (b). (c) PFM phase difference measured along the white line in (a). (d) PFM amplitude as a function of the loading force extracted from cross-section analysis of the white line in (c). (e) Mechanically written domain lines with a tip under loading force from 80 to 400 nN. (f) Cross-sectional line profile of the domain written with $F_L = 100$ nN. The estimated domain line width w_m is 8.9 nm.

(Fig. 1) and could enable mechanical writing of ultradense ferroelectric nanodomains.

Figure 3(e) shows downward-polarization domain lines, which we mechanically write by scanning the CaTiO_3 film with a tip under several different F_L . With $F_L \geq 100$ nN, a domain line is perfectly writable and remains stable for at least several hours. From the cross-sectional line profile of the domain written with $F_L = 100$ nN [Fig. 3(f)], we determine the minimum domain width w_m achievable by mechanical writing. This yields a mean of $w_m = 9.4 \pm 1.3$ nm, suggesting an ultrahigh recording density of ≥ 1 Tbit cm^{-2} (extrapolated from the individual domain size of 9.4×9.4 nm 2). Therefore, our CaTiO_3 promises a markedly improved domain density, compared with previous studies [e.g., $w_m = 30$ nm, corresponding to around 110 Gbit cm^{-2} , in $\text{Pb}(\text{Zr}, \text{Ti})\text{O}_3$] [34].

Mechanically written, ~ 10 nm-wide FE domains remain quite stable for a long time, without any noticeable change in the PFM phase profile [Figs. 4(a) and 4(b)]. PFM signals (or amplitudes) usually decay, following a power-law $P(t) \propto t^{-\alpha}$ with a decay exponent α . Referring to the α value [Fig. 4(c)], mechanically written, < 10 nm-wide domains of 5 nm-thick CaTiO_3 film seems to have

good stability ($\alpha = 0.11$), even slightly better than that ($\alpha = 0.12$) of electrically written, a few micrometers-wide domains of 5 nm-thick BaTiO_3 film [42]. We also find that the nanoscale array of dot-shaped domains is stable over time (Fig. S9 [22]). These results support that high-density nanoscale domains of metastable ferroelectrics can remain stable once mechanically written.

The key parameters for assessing mechanical polarization switching are its threshold F_L and the achievable density of the written nanodomains. We combine these two factors by defining a figure of merit as $1/(F_{L,\text{th}} \times w_m^2)$, where $F_{L,\text{th}}$ is the threshold F_L . Since a low $F_{L,\text{th}}$ and a small w_m^2 have been incompatible with each other, the reciprocal of their product could be a suitable figure of merit. Based on this, we compare the performance of mechanical polarization switching of our CaTiO_3 (111) films with those of other ferroelectric perovskite oxides (details in Supplemental Material Note G, Table S1 [22]). In particular, for an appropriate comparison, we grow BaTiO_3 (001) and (111) films and then examine their mechanical polarization switching using the same experimental setup as for CaTiO_3 . Also, all samples in comparison have a similar thickness of 5 nm. Figure 5 shows

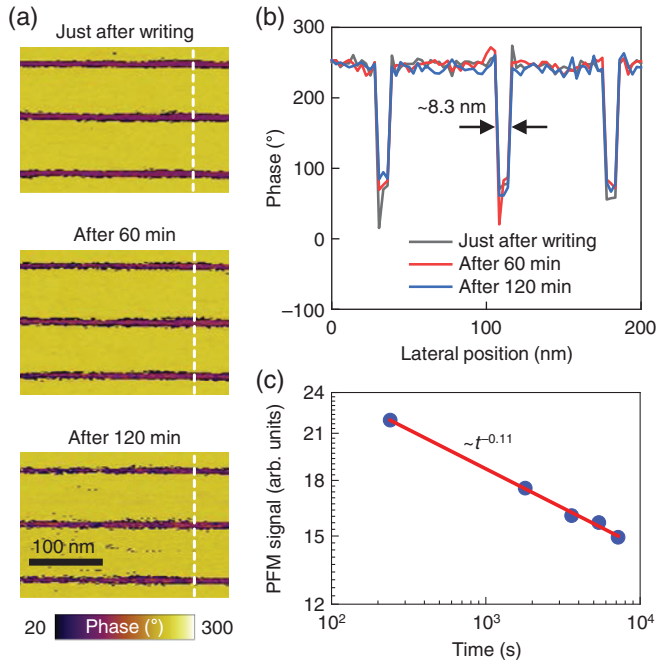


FIG. 4. Stability of mechanically written ferroelectric domains on 5 nm-thick CaTiO_3 film. (a) PFM phase images of mechanically written line domains, measured just after domain writing, 60 min later, and 120 min later. Line domains are mechanically written with $F_L \sim 100$ nN. (b) PFM phase difference measured along the white dashed lines in (a). The estimated width of line domains is around 8.3 nm. (c) PFM signal (or amplitude) measured as a function of time after domain writing. Red solid line is fit to the power-law decay $P(t) \propto t^{-\alpha}$, where the decay exponent α is estimated as small as 0.11.

that our CaTiO_3 exhibits a greatly enhanced figure of merit, as well as markedly reduced threshold F_L , compared with other ferroelectrics. As proposed, this enhanced performance of mechanical polarization switching could originate from the unique mechanical response of metastable ferroelectricity. Therefore, we demonstrate the feasibility of a new strategy exploiting metastable ferroelectricity to realize hyper-efficient mechanical polarization switching.

Thanks to advances in experimental and theoretical techniques, recent studies have revealed that metastable ferroelectricity could occur commonly in complex materials, such as BiFeO_3 and HfO_2 . In BiFeO_3 , many competing phases, such as tetragonal-like phase, rhombohedral phase, and the mixed phase, have emerged, e.g., when it is epitaxially strained [13,43]. Some of the competing phases are ferroelectric, so that the actual polarization switching process could be accompanied with rich phase transformations, and the consequent elastic softening might beneficially improve the efficiency of polarization switchings. On the other hand, CaTiO_3 contains only the two states (i.e., $Pnma$ and $R3c$) that simply govern the polarization switching process under an applied electric (or flexoelectric) field. Thanks to this simplicity, the minimal

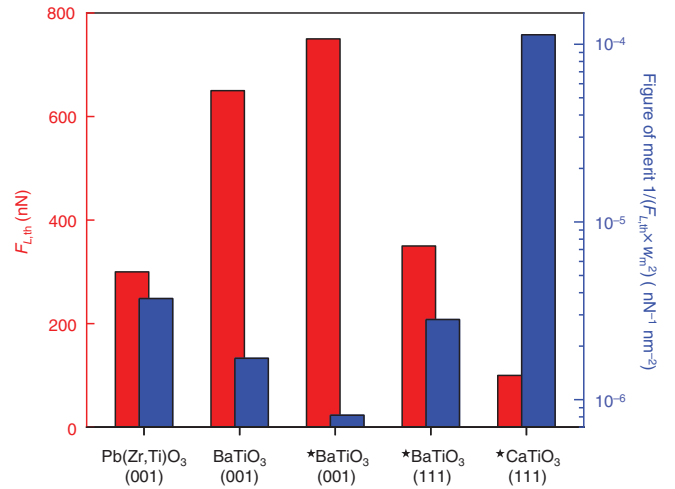


FIG. 5. Mechanical polarization switching of CaTiO_3 and other ferroelectric perovskite oxides. Those marked with star denote samples that we grow, for which mechanical switching is investigated with the same experimental setup. The values of threshold loading forces ($F_{L,\text{th}}$) and minimum widths (w_m) of mechanically written domains for $\text{Pb}(\text{Zr}, \text{Ti})\text{O}_3$ and BaTiO_3 are acquired from Refs. [34] and [12], respectively.

Landau free energy could successfully explain the experimentally studied mechanical polarization switching in CaTiO_3 (Fig. 1). Another interesting system, i.e., an HfO_2 thin film, has the nonpolar ground state and the ferroelectric metastable state, quite similar to our CaTiO_3 (111) films. Possibly, due to this similarity, an HfO_2 thin film also exhibited a low threshold loading force as small as 100 nN for mechanical polarization switching [44]. Although the previous work on HfO_2 did not explicitly examine the high-density domain writing and the critical role of metastable ferroelectricity, it suggests that the unique mechanical response of the “detour-switching path” could generally be present in metastable ferroelectricity. We believe that our approach could be generally applicable to a variety of metastable ferroelectric systems that have recently been in the spotlight.

Our study reveals a genuinely intrinsic aspect of mechanical polarization switching, which has both scientific and technological implications. Newly employing metastable ferroelectricity, we maximize the beneficial role of AFM tip-induced strain to reduce the threshold F_L for polarization switching. The use of low F_L would also reduce damage to both sample and tip, thereby promising more reliable and reproducible mechanical polarization switching. Rather surprisingly, despite chemical and structural similarities, our CaTiO_3 exhibits distinctly superior mechanical polarization switching, compared with other perovskite oxides. This underlines the rich physics behind mechanical polarization switching; the efficiency of mechanical polarization switching could be sensitive to the detailed characteristics of ferroelectricity (e.g., whether it is stable or metastable, as in this study). Moreover, AFM tip-induced strain can be useful

not only for mechanical polarization switching but also generally for controlling local free energy landscapes in complex materials. Therefore, our study suggests another opportunity to access exotic metastable quantum states and even write them locally at the nanoscale.

This work was supported by the Research Center Program of the Institute for Basic Science (IBS) in Korea (IBS-R009-D1) and by the National Research Foundation of Korea (NRF) grant funded by the Korea government (MSIT) (No. 2019R1C1C1002558 and No. 2021R1A5A1032996). This work was supported by Samsung Electronics Co., Ltd (IO201211-08061-01). This paper is supported by Basic Science Research Institute Fund, whose NRF grant number is 2021R1A6A1A10042944. S. Y. P. was supported by the National Research Foundation of Korea (NRF) grant funded by the Korea government (MSIT) (No. 2021R1C1C1009494) and by Basic Science Research Program through the National Research Foundation of Korea (NRF) funded by the Ministry of Education (No. 2021R1A6A1A03043957).

J. H. L., H. J. K., and J. Y. contributed equally to this work.

*Corresponding author.

jihye33@gmail.com

†Corresponding author.

sp2829@ssu.ac.kr

‡Corresponding author.

dlee1@postech.ac.kr

- [1] M. Lines and A. Glass, *Principles and Applications of Ferroelectrics and Related Materials* (Clarendon Press, Oxford, UK, 2001).
- [2] R. V. Wang, D. D. Fong, F. Jiang, M. Highland, P. H. Fuoss, C. Thompson, A. M. Kolpak, J. A. Eastman, S. K. Streiffer, A. M. Rappe, and G. B. Stephenson, Reversible Chemical Switching of a Ferroelectric Film, *Phys. Rev. Lett.* **102**, 047601 (2009).
- [3] Z. Wen, C. Li, D. Wu, A. Li, and N. Ming, Ferroelectric-field-effect-enhanced electroresistance in metal/ferroelectric/semiconductor tunnel junctions, *Nat. Mater.* **12**, 617 (2013).
- [4] S. H. Baek, H. W. Jang, C. M. Folkman, Y. L. Li, B. Winchester, J. X. Zhang, Q. He, Y. H. Chu, C. T. Nelson, M. S. Rzechowski, X. Q. Pan, R. Ramesh, L. Q. Chen, and C. B. Eom, Ferroelastic switching for nanoscale non-volatile magnetoelectric devices, *Nat. Mater.* **9**, 309 (2010).
- [5] H.-J. Lee, M. Lee, K. Lee, J. Jo, H. Yang, Y. Kim, S. C. Chae, U. Waghmare, and J. H. Lee, Scale-free ferroelectricity induced by flat phonon bands in HfO₂, *Science* **369**, 1343 (2020).
- [6] X. Xu, Y. Wang, F. T. Huang, K. Du, E. A. Nowadnick, and S. W. Cheong, Highly tunable ferroelectricity in hybrid improper ferroelectric Sr₃Sn₂O₇, *Adv. Funct. Mater.* **30**, 2003623 (2020).
- [7] S. Li and T. Birol, Suppressing the ferroelectric switching barrier in hybrid improper ferroelectrics, *npj Comput. Mater.* **6**, 168 (2020).
- [8] S. M. Kogan, Suppressing the ferroelectric switching barrier in hybrid improper ferroelectrics, *Sov. Phys. Solid State* **5**, 2069 (1964).
- [9] P. Zubko, G. Catalan, A. Buckley, P. R. L. Welche, and J. F. Scott, Strain-Gradient-Induced Polarization in SrTiO₃ Single Crystal, *Phys. Rev. Lett.* **99**, 167601 (2007).
- [10] D. Lee, S. Y. Yoon, J.-G. Jang, J.-S. Yoon, M. Chung, M. Kim, J. F. Scott, and T. W. Noh, Giant Flexoelectric Effect in Ferroelectric Epitaxial Thin Films, *Phys. Rev. Lett.* **107**, 057602 (2011).
- [11] P. Zubko, G. Catalan, and A. K. Tagantsev, Flexoelectric effect in solids, *Annu. Rev. Mater. Res.* **43**, 387 (2013).
- [12] H. Lu, C.-W. Bark, D. Esque de los Ojos, J. Alcala, C. B. Eom, G. Catalan, and A. Gruverman, Mechanical writing of ferroelectric polarization, *Science* **336**, 59 (2012).
- [13] K. Chu, B.-K. Jang, J. H. Sung, Y. A. Shin, E.-S. Lee, K. Song, J. H. Lee, C.-S. Woo, S. J. Kim, S.-Y. Choi, T. Y. Koo, Y.-H. Kim, S. H. Oh, M. H. Jo, and C.-H. Yang, Enhancement of the anisotropic photocurrent in ferroelectric oxides by strain gradients, *Nat. Nanotechnol.* **10**, 972 (2015).
- [14] U. K. Bhaskar, N. Banerjee, A. Abdollahi, Z. Wang, D. G. Schlom, G. Rijnders, and G. Catalan, A flexoelectric microelectromechanical system on silicon, *Nat. Nanotechnol.* **11**, 263 (2016).
- [15] M.-M. Yang, D. J. Kim, and M. Alexe, Flexo-photovoltaic effect, *Science* **360**, 904 (2018).
- [16] S. Das, B. Wang, T. R. Paudel, S. M. Park, E. Y. Tsymlal, L.-Q. Chen, D. Lee, and T. W. Noh, Enhanced flexoelectricity at reduced dimensions revealed by mechanically tunable quantum tunneling, *Nat. Commun.* **10**, 537 (2019).
- [17] L. Wang, S. Liu, X. Feng, C. Zhang, L. Zhu, J. Zhai, Y. Qin, and Z. L. Wang, Flexoelectronics of centrosymmetric semiconductors, *Nat. Nanotechnol.* **15**, 661 (2020).
- [18] L. J. McGilly, A. Kerelsky, N. R. Finney, K. Shapovalov, E.-M. Shih, A. Ghiotto, Y. Zeng, S. L. Moore, W. Wu, Y. Bai, K. Watanabe, T. Taniguchi, M. Stengel, L. Zhou, J. Hone, X. Zhu, D. N. Basov, C. Dean, C. E. Dreyer, and A. N. Pasupathy, Visualization of moiré superlattices, *Nat. Nanotechnol.* **15**, 580 (2020).
- [19] X. Chen, X. Tang, X.-Z. Chen, Y.-L. Chen, X. Guo, H.-X. Ge, and Q.-D. Shen, Nonvolatile data storage using mechanical force-induced polarization switching in ferroelectric polymer, *Appl. Phys. Lett.* **106**, 042903 (2015).
- [20] S. M. Park, B. Wang, S. Das, S. C. Chae, J.-S. Chung, J.-G. Yoon, L.-Q. Chen, S. M. Yang, and T. W. Noh, Selective control of multiple ferroelectric switching pathways using a trailing flexoelectric field, *Nat. Nanotechnol.* **13**, 366 (2018).
- [21] P. Sharma, S. Ryu, Z. Viskadourakis, T. R. Paudel, H. Lee, C. Panagopoulos, E. Y. Tsymlal, C. B. Eom, and A. Gruverman, Electromechanics of ferroelectric-like behavior of LaAlO₃ thin films, *Adv. Funct. Mater.* **25**, 6538 (2015).
- [22] See Supplemental Material at <http://link.aps.org/supplemental/10.1103/PhysRevLett.129.117601> for methods and supplemental data, which includes Refs. [23–32].
- [23] D. M. Ceperley and B. J. Alder, Ground State of The Electron Gas by a Stochastic Method, *Phys. Rev. Lett.* **45**, 566 (1980).
- [24] J. P. Perdew and A. Zunger, Self-interaction correction to density-functional approximations for many-electron systems, *Phys. Rev. B* **23**, 5048 (1981).

- [25] G. Kresse and J. Furthmüller, Efficient iterative schemes for *ab initio* total-energy calculations using a plane-wave basis set, *Phys. Rev. B* **54**, 11169 (1996).
- [26] G. Kresse and D. Joubert, From ultrasoft pseudopotentials to the projector augmented-wave method, *Phys. Rev. B* **59**, 1758 (1999).
- [27] P. E. Blöchl, Projector augmented-wave method, *Phys. Rev. B* **50**, 17953 (1994).
- [28] R. D. King-Smith and D. Vanderbilt, Theory of polarization of crystalline solids, *Phys. Rev. B* **47**, 1651(R) (1993).
- [29] M.-M. Yang, D. J. Kim, and M. Alexe, Flexo-photovoltaic effect, *Science* **360**, 904 (2018).
- [30] A. P. Sakhya, Electronic structure and elastic properties of ATiO_3 ($A = \text{Ba, Sr, Ca}$) perovskites: A first principles study, *Indian J. Pure Appl. Phys.* **53**, 102 (2015).
- [31] Y. Gu, K. Rabe, E. Bousquet, V. Gopalan, and L. Q. Chen, Phenomenological thermodynamic potential for CaTiO_3 single crystals, *Phys. Rev. B* **85**, 064117 (2012).
- [32] B. Wang, H. Lu, C. W. Bark, C.-B. Eom, and A. Gruverman, Mechanically induced ferroelectric switching in BaTiO_3 thin films, *Acta Mater.* **193**, 151 (2020).
- [33] A. C. Fischer-Cripps, *Introduction to Contact Mechanics* (Springer, New York, USA, 2007).
- [34] E. J. Guo, R. Roth, S. Das, and K. Dorr, Strain induced low mechanical switching force in ultrathin $\text{PbZr}_{0.2}\text{Ti}_{0.8}\text{O}_3$ films, *Appl. Phys. Lett.* **105**, 012903 (2014).
- [35] Z. Wen, X. Qiu, C. Li, C. Zheng, X. Ge, A. Li, and D. Wu, Mechanical switching of ferroelectric polarization in ultrathin BaTiO_3 films: The effects of epitaxial strain, *Appl. Phys. Lett.* **104**, 042907 (2014).
- [36] J.-H. Liu, X. Chen, Y. Li, X. Guo, H.-X. Ge, and Q.-D. Shen, Ferroelectric polymer nanostructure with enhanced flexoelectric response for force-induced memory, *Appl. Phys. Lett.* **113**, 042903 (2018).
- [37] A. K. Tagantsev, Size effects in polarization switching in ferroelectric thin films, *Integr. Ferroelectr.* **16**, 237 (1997).
- [38] J. R. Kim, J. Jang, K.-J. Go, S. Y. Park, C. J. Roh, J. Bonini, J. Kim, H. G. Lee, K. M. Rabe, J. S. Lee, S.-Y. Choi, T. W. Noh, and D. Lee, Stabilizing hidden room-temperature ferroelectricity via a metastable atomic distortion pattern, *Nat. Commun.* **11**, 4944 (2020).
- [39] W. Ostwald, Studien über die Bildung und Umwandlung fester Körper, *Z. Phys. Chem.* **22**, 289 (1897).
- [40] Y. Qi, S. Singh, C. Lau, F.-T. Huang, X. Xu, F. J. Walker, C. H. Ahn, S.-W. Cheong, and K. M. Rabe, Stabilization of Competing Ferroelectric Phases of HfO_2 Under Epitaxial Strain, *Phys. Rev. Lett.* **125**, 257603 (2020).
- [41] M. Vopsaroiu, J. Blackburn, M. G. Cain, and P. M. Weaver, Thermally activated switching kinetics in second-order phase transition ferroelectrics, *Phys. Rev. B* **82**, 024109 (2010).
- [42] D. Lee, H. Lu, S.-Y. Choi, S.-D. Li, S. Ryu, T. R. Paudel, K. Song, E. Mikhnev, S. Lee, S. Stemmer, D. A. Tenne, S. H. Oh, E. Y. Tsybal, X. Wu, L.-Q. Chen, A. Gruverman, and C. B. Eom, Emergence of room-temperature ferroelectricity at reduced dimensions, *Science* **349**, 1314 (2015).
- [43] Y. Heo, B.-K. Jang, S. J. Kim, C.-H. Yang, and J. Seidel, Nanoscale mechanical softening of morphotropic BiFeO_3 , *Adv. Mater.* **26**, 7568 (2014).
- [44] U. Celano, M. Popovici, K. Florent, S. Lavizzari, P. Favia, K. Paulussen, H. Bender, L. di Piazza, J. V. Houdt, and W. Vandervorst, The flexoelectric effect in Al-doped hafnium oxide, *Nanoscale* **10**, 8471 (2018).